Published in: Journal of the European Ceramic Society 30 (2010) 147–152
doi:10.1016/j.jeurceramsoc.2009.04.031

Compositionally graded YSZ-NiO composites by surface laser melting

Rosa I. Merino[a], J.I. Peña [b] and V.M. Orera[a]

Instituto de Ciencia de Materiales de Aragón

[a] Departamento de Física de la Material Condensada

[b] Departamento de Ciencia y Tecnología de Materiales y Fluidos

CSIC-Universidad de Zaragoza, 50009 Zaragoza, Spain

Presented at ELECTROCERAMICS XI, A-013-I

Abstract

Laser surface melting has been applied to near eutectic NiO-YSZ sintered ceramics. The objective is to generate a functional gradient composite material with graded microstructure and composition. At low solidification rates the resultant material has a graded composition, with a severe NiO segregation towards the surface. A thick NiO layer whose thickness depends on the travelling speed is formed. Below this layer the microstructure is eutectic like with composition varying with depth. In contact with the ceramic, excess YSZ coming from the hyper-eutectic composition forms an almost continuous YSZ layer. The thickness of both segregated layers, NiO and YSZ can be controlled by traverse speed. Thickness decreases as travelling speed increases until a limiting travelling rate of 110 mm/h, at which no more segregation is found. Possible causes to explain the relevant NiO segregation toward the surface are discussed.

KEYWORDS: NiO, YSZ, eutectics, laser surface melting, functional gradient material.

Published in: Journal of the European Ceramic Society 30 (2010) 147–152
doi:10.1016/j.jeurceramsoc.2009.04.031

1. Introduction

The fabrication of in-situ composites by solidification of oxide eutectics (DSEO) has been the subject of strong attention in the last decade due to the excellent mechanical properties they presented. This is particularly true for the eutectics with Al_2O_3 as a component and with fine and homogeneous microstructure.[1,2,3,4] Directional solidification allows size control over the final microstructure, and being that an advantage, other applications different than the structural ones have been proposed: single crystalline porous matrix[5], photonic materials [6] or metal-ceramic composites with particularly stable interphases[7].

Laser melt processing of materials is also a well-known subject among technologist and material scientist working with metals[8]. Its application to ceramics is scarcer [9,10,11] as ceramics tend to be fragile, and special attention has to be paid to handle the processing thermal stresses. The procedure we are interested in generates a surface dense crystallised eutectic composite on top of a dense[11] or porous[12] eutectic ceramic, with the same or different composition[13]. Applications of the procedure exist in all areas where dense and smooth thick ceramic covering layers are required: erosion and abrasion resistance, wear resistance, etc. Other modifications as in surface tube remelting, can be used to generate different geometries, useful for example to produce filter tubes with enhanced surface catalytic activity (due to its nanometer size porous microstructure [14]).

Surface remelting of eutectic oxides results normally in a graded microstruture[10,12] with average homogeneous composition. Sometimes, however, we have observed macroscopic segregation. For example, in laser surface rmelting of $CaZrO_3$-CaSZ eutectic at 100 mm/h,[15] a $CaZrO_3$ single-phase surface layer is observed, accompanied by a graded composition below it. It goes from 100 vol% $CaZrO_3$ at the surface to an eutetic like microstructure 62 vol% $CaZrO_3$ – 38vol% CaO stabilized ZrO_2 at 200 □m below the surface and down to the ceramic. A similar behaviour was observed by Yoshikawa et al.[16] on Al_2O_3-YAG thin fibers produced by the micropulling down method. They report a self-cladding of YAG on the Al_2O_3-YAG core eutectic. When solidifying slightly YSZ-rich YSZ-Al_2O_3 hypereutectics, we have observed that the first solid phase to deposit at the interface with the ceramic is YSZ. Size and compositionally graded materials have also been found in the realization of laser cladding and laser alloying of metals [17,18].

In the following we present the results of the surface laser melt processing of YSZ-NiO near eutectic ceramics at different solidification rates. The starting composition was slightly enriched in YSZ to generate a continuous dense YSZ electrolyte layer separating the porous ceramic substrate from the

Published in: Journal of the European Ceramic Society 30 (2010) 147–152
doi:10.1016/j.jeurceramsoc.2009.04.031

composite resolidified layer. The objective of this work is primarily to establish the conditions upon which a graded composition is attained for this mixture and explore its physical origin. The second objective is to evaluate its applicability as a single-step procedure to create eutectic - thin YSZ - eutectic three layer structure for possible uses, particularly in the field of solid oxide fuel cells.

2. Experimental details.

Porous ceramic plates were prepared by colloidal processing. Starting powders of NiO (99.99% from Aldrich) were attrition milled for 5h in isopropanol with zirconia milling balls. 58.28 wt% of this NiO powder and 41.72 wt % YSZ (yttria-stabilized zirconia) from Tosoh (TZ-8YS, grain size 0.25 □m) were mixed and an extra 1.8 wt % graphite powder (Alpha Aesar 99%, particle size < 45 □m) added to create porosity, and dry mixed. The powder mixture was added to a solution prepared with H_2O and ethanol as solvents and PVA (15000 molecular weight, 81381 Fluka). The suspension was stirred and ultrasonicated several times. Finally, the slurry was slip cast on to plaster moulds, allowed to dry overnight, and then sintered. The ceramic plate thickness was from 2 to 3.6 mm, and cut to stripes around 7 mm width. Final density was 80 %. The microstructure of the ceramic consists of fine and dispersed grains of NiO and YSZ, as well as dual porosity.

Laser surface melting was performed with a high power diode laser from Rofin-Sinar (940 nm wavelength) as described elsewhere[11]. The sample was preheated by placing it on a metallic support that was kept at 1080 ºC during processing. An almost homogeneous intensity laser line with size w_x = 10mm (along X direction) and w_y = 1 mm (along Y direction) is focussed on the surface of the sample that travelled along the Y direction at a fixed traverse speed. Laser powers of 60 to 70 W were used (that is, fluences of 600 to 700 W/cm^2), and traverse speeds from 10 mm/h to 500 mm/h.

Scanning electron microscopy was used to observe the samples microstructure, using a JEOL 6400 Scanning Electron Microscope (SEM) equipped with a Link Analytical X-ray detector for microanalysis by Energy Dispersive Spectroscopy (EDS).

3. Results

3.1. Microstructure.

Published in: Journal of the European Ceramic Society 30 (2010) 147–152
doi:10.1016/j.jeurceramsoc.2009.04.031

In figure 1 we give SEM micrographs of transverse (XZ) polished cross-sections of samples processed at increasing laser scanning rates from 20 mm/h to 500 mm/h. At rates below 100 mm/h, primary YSZ (bright phase) has nucleated and deposited near to the interface with the unmelted, underlaying ceramic; and a layer of NiO (dark phase) has been formed on the free upper surface. The thickness of these single-phase layers increases as processing rate decreases. A closer view of the upper layer is presented in Figure 2 for two slow processing rates. One can observe that below the single phase NiO layer (perhaps containing YSZ traces), the composition is also graded with a microstructure that consist of YSZ fibers for the first 20 μm and then, as NiO content increases, converts into lamellar eutectic grains. At 500 mm/h no depth (Z)-dependent segregation can be appreciated on the micrographs. Instead, primary YSZ dendrites start to grow and project towards the melt because of constitutional undercooling at this processing rate of an intentionally YSZ rich mixture.

In table 1 we give values of the thickness of each single-phase layer as well as of the full-solidified layer. Laser power densities were adjusted so that the total thickness stayed on a narrow range around 400 μm. Adjacent to the ceramic, YSZ formed an apparently continuous layer at the lowest solidification rates, although cracks progress along this layer. The cracks were formed because upon solidifying and cooling of the upper layer, this one stays subjected to tensile stress directed along the width of the sample. One way to relax this stress state is to delaminate and separate from the ceramic. Single phase YSZ is less tough than the dual phase porous ceramic or solidified eutectic, and consequently fails. Upon increasing the solidfication rate, the thickness of the YSZ layer decreases and eventually the delamination disappears. The transition between cracked and non-cracked interface is observed at around 60 mm/h, were rare delamination cracks are observed and the YSZ layer apparently is continuous with 7 micron thickness.

3.2. Composition.

The NiO layer (of thickness δ_n) contained less than 0.5 % Zr cations. The composition from the steep frontier between NiO towards the inside is given in figure 3 as a function of position inside the layer normalized to (δ_t-δ_n). δ_t is the total thickness of the solidified layer. The composition goes from Ni rich for z-$\delta_n \rightarrow 0$, to Ni poor, with a decay length that increases as we decrease solidification rate. The decay curves that result from an exponential fit to the experimental data are shown in the image with continuous lines. The composition of the ceramic, as measured also by EDS, is shown by a discontinuous line (66±1 at%Ni) for reference.

Published in: Journal of the European Ceramic Society 30 (2010) 147–152
doi:10.1016/j.jeurceramsoc.2009.04.031

Decay lengths as well as the thickness of the fully segregated single phase layers indicate that, as the traverse speed decreases (decrease in solidification rate), the total amount of segretated Ni in the solid increases, either in the form of isolated phase or as eutectic like regions of increased NiO content. Both magnitudes are plotted jointly in figure 4 as a function of traverse speed. Both extrapolate to a traverse speed rate of around 110 mm/h to cancel out the segregation.

The fact that the slower the solidification rate, the stronger the segregation, points to a diffusion process into the liquid as its origin, in a way that, the more time is available for the Ni to diffuse in the melt (slow solidification rates), the more it segregates towards the surface. Consequently, we have also explored the melt composition in the following way. We have stopped one solidification-run at 20 mm/h by switching off the laser, and looked at the frozen-melt composition on a longitudinal cross-section at the centreplane. In figure 5 we give the longitudinal cross section with indication of the position where cation microanalysis was done. In figure 3 we have also included with stars the Ni content measured in this frozen melt along this line distant 10 to 20 μm from the solidification front. The composition of the quenched melt is 73.1 at% Ni, with small dispersion at this position (σ_d = 0.55). This is to be compared with the true eutectic composition (73.5 at %Ni, [19]). A small deviation from this composition is found at the last to solidify center side of the drop (70.3 at %), where bright dendrites are seen. However, looking at the frozen melt in average, it appears that its average composition is shifted from the initial one towards the true eutectic

3.3 YSZ layer tightness

In order to test the usefullnes of the YSZ layer as a barrier between the YSZ-NiO composites (ceramic and solidified eutectic), we took a 5x5 mm^2 piece of sample prepared at 60 mm/h (which shows no delamination); treated it at 800 ºC in 5%H_2-N_2 mixture to reduce NiO to metallic Ni and measured the conductivity across the sample. The sample withstood the treatment without delamination or cracking, although it turned out that some electronic leak current crossed the YSZ layer. Since the conductivity was metallic like (with resistivity increasing with temperature), the most probable cause is that metallic Ni wires that result form the reduction of NiO to Ni, cross the YSZ layer which was probably continuous but drilled at some places by NiO bridges connecting both sides of the membrane. In fact, in figure 1a, NiO wires or films can be observed surrounding many of the primary zirconia particles that have nucleated and grown on top of the ceramic. This suggest that full tightness of the YSZ layer is hardly to achieve by such a solidification process, even if delamination were avoided. Only relatively thick YSZ layers could eventually be considered free of leaks.

Published in: Journal of the European Ceramic Society 30 (2010) 147–152
doi:10.1016/j.jeurceramsoc.2009.04.031

4. Discussion.

The formation of the primary YSZ layer at the bottom of the layer can be understood as a consequence of constitutional undercooling caused by the off-eutectic solidification [20,21]. The appearance of the large macroscopic segregation of NiO is more difficult to explain.

First we consider than strong thermal gradients are developed at the stage of laser processing by surface melting [22], where a high energy density is deposited onto the surface of the material. At the surface, the melt overheats some hundred Kelvin above melting point (T_m) , whereas around 400 □m below the solid-liquid interface stays at T_m. These large thermal gradients cause strong convection flows. Different authors [22,23] have calculated them. From studies on the melt processing of metals, the larger liquid velocity takes place at the surface of the liquid where there is a strong Marangony convection. Convection flow goes at the surface from the centre of the melt pool towards the sides. Buoyancy helps to close the loop with upward flow in the middle of the melt pool and sinking fluid in front of the solid-liquid interface. We can roughly estimate the order or magnitude of convection currents in our melt using the results given by Kou[24], for an aluminun alloy and assuming that the maximun velocity is linearly proportional to melt pool size, thermal gradient, and surface tension slope ($d\gamma/dT$) and inversely proportional to viscosity (μ). If we take: $d\gamma/dT = -3.5\ 10^{-5}$ N/mK, and μ = 46 cP as in YAG [25]; and thermal gradient = 700 K/mm [21], we estimate a maximum velocity at the surface of 1 mm/s. This is much larger than the solidification rate and shows that the melt is strongly stirred and mixed, which results in a rather homogeneous composition, as observed by the EDS analyses of the frozen melt. If macroscopic inhomogeneities would exist in this melt, they would be seen on the frozen melt. So, we can exclude the existence of a thick layer (around 100 □m) of NiO on top of the melt. Consequently, to transfer the observed big segregation of NiO to the solidifying composite out of a rather homogeneous melt, it is of importance what is happening at the very solid-liquid interface.

The convection currents feed the solid-liquid interface with liquid from the surface of the melt pool and downwards. If they are fast enough and are able to penetrate the diffusion boundary layer (wider as the solidification rate decreases), the matter they transport may be deposited into the solid as it reaches the advancing solidification front. Let us assume that there is a thin NiO rich layer at the surface of the melt, without inquiring ourselves of its origin for the moment. An estimate of the thickness of this upper NiO rich layer (δ) can be done if one assumes that all this NiO located between the centre of the melt pool and the solidification front is incorporated into the single phase NiO solidified layer. That is, we are not

Published in: Journal of the European Ceramic Society 30 (2010) 147–152
doi:10.1016/j.jeurceramsoc.2009.04.031

considering losses of NiO from subsequent mixing in the melt or the NiO fraction that has reached larger depths at the solid-liquid interface. Conservation of NiO mass requires that the NiO mass deposited per unit time per unit length of the solidification front equals the mass transported by convection (at velocity V_c) towards this surface:

$$\delta_n \rho_s R = \delta \rho_l V_c \qquad (1)$$

R is the travelling rate, ρ_s and ρ_l are the mass density of solid and liquid NiO respectively. Using the values given in table 1, neglecting mass density differences between solid an liquid, and taking V_c = 1mm/s, we estimate a NiO layer thickness on the melt of 200 to 480 nm thick in our experiments. Of course, □ will depend on the processing parameters and on the mechanism by which this layer is fed with Ni coming from a small volume of melt that, moreover, becomes poor in Ni by the process. The preceding estimate does however tell us that the NiO layer thickness required to account for the observed segregation is very small, less than 1 micron, and would account for much of the δ_n vs. traverse speed dependence presented in figure 4.

There are several possible mechanisms for composition inhomogeneity in an inhomogeneously heated melt with an advancing solidification front. There may be solutal and thermosolutal convection (when the density variations are generated by different solute content)[22]. But solid NiO is denser than solid YSZ, and we have no hints that would suggest the same is not true for their melts. Liquid NiO would sink. Moreover, experiments on vertical LFZ growth of NiO-YSZ eutectics pulling the crystal downwards[19] still present preferential segregation towards the surface, which is in contradiction. In the absence of convection, thermal gradients can also produce the migration of species by a diffusion process (thermotransport or Soret Effect), causing the cold and hot regions of the liquid to be richer in one or the other species forming the mixture [26]. It there were preferential diffusion of NiO towards the hottest melt regions, NiO would migrate towards the top of the melt. Changes in composition arise also in the diffusion layer as well as in the mushy zone[27] when a solute has partition coefficient different from 1, although one would not expect this to be the case in the solidification of a eutectic. Liquid-gas interaction might be able to segregate a very thin layer of NiO at the surface. Surface tension and stoichiometry of both liquid oxides and its mixtures can be very different.

Unfortunately, there are no data in the literature about liquid densities, its dependence on stoichiometry, thermodiffuson coefficients of cations in the mixture or surface tension values that would allow estimate rates of segregation to compare with the experiments. Our experimental evidence alone is not enough

to propose one mechanism with much preference. More experiments with varying conditions and with different systems are needed to identify the precise mechanism of the severe NiO segregation.

5. Conclusions

We have proved that applying surface laser melting to YSZ rich hypereutectic of YSZ-NiO ceramics, a layered material consisting of the following layers: composite ceramic (2 to 3 mm), primary zirconia (around 10 μm), eutectic with graded compositon (around 400 μm) and single-pahse NiO (approximately 30 μm thick), is formed. This can be done at solidification rates between 20 and 100 mm/h. The thickness of the fully segregated layers (YSZ and NiO) increases as the laser scanning rate decreases.

To use this procedure to prepare ceramic functional gradient materials (FGM), thermal stresses have to be carefully handled. Very thick, single phase YSZ separating the resolidified layer and the supporting ceramic might not be attained because of them fracturing this fragile layer.

The most relevant result of the work is the macroscopic segregation of NiO towards the surface, which even forms a thick layer. Although we were not able to identify the mechanism, the experiments suggest that interaction of the melt with the surrounding gas or thermal diffusion of the NiO towards the hottest areas of the melt might be playing a role in the process. Further research is needed to fully understand it, which will allow apply the procedure to different eutectic mixtures to create FGM by laser surface melting as well as by laser floating zone eutectic growth.

Acknowledgments

We thank M.A. Laguna-Bercero for his help in the SEM experiments. Finantial support from the Ministerio de Educación y Ciencia of Spain and the CE program FEDER under grant MAT2006-13005-C03-01 is gratefully acknowledged.

Published in: Journal of the European Ceramic Society 30 (2010) 147–152
doi:10.1016/j.jeurceramsoc.2009.04.031

References

1.- Sayir, A., Farmer, SC. The effect of microstructure on mechanical porperties of directionally solidified $Al_2O_3/ZrO_2(Y_2O_3)$eutectic. *Acta Mater*, 2000, **48**, 4691-4697

2.- Waku, Y., Nakagawa, N., Wakamoto, T., Ohtsubo, H., Shimizu, K.and Kohtoku, Y.,

A ductile ceramic eutectic composite with high strength at 1873 K *Nature* (London), 1997, **389**, 49–52.

3.- Lee, JH., Yoshikawa, A., Murayama, Y., Waku, Y., Hanada, S. and Fukuda, T. Microstructure and mechanical properties of $Al_2O_3/Y_3Al_5O_{12}/ZrO_2$ ternary eutectic materials. *J. Europ. Ceram. Soc*. 2005, **25**, 1411-1417.

4.- Oliete, P.B., Peña, J.I., Larrea, A., Orera, V.M., LLorca, J., Pastor, J.Y., Martín, A., and Segurado, J. Ultra-High-Strength Nanofibrillar Al_2O_3–YAG–YSZ Eutectics. *Adv.Mater*. 2007, **19**, 2313 –2318.

5.- Larrea, A. and Orera, V.M. Porous crystal structures obtained from directionally solidified eutectic precursors. *Journal of Crystal Growth* 2007, **300**, 387-393.

6.- Orera, V.M. Larrea, A., Merino, R.I., Rebolledo, M.A., Vallés, J.A., Gotor, R. and Peña, J.I. Novel photonic materials made form ioinic eutectic compounds. *Acta Physica Slovaca* **55** (2005) 261-269.

7.- Laguna-Bercero, M.A. and Larrea, A. YSZ-Induced Crystallographic Reorientation of Ni Particles in Ni–YSZ Cermets, *J. Am. Ceram. Soc*., 2007, **90**, 2954 –2960.

8.- Steen, W.M. *Laser Material Processing*, Springer-Verlag. London, 2003.

9.- Triantafyllidis, D., Li, L. and Stott, F.H. Crack free densification of ceramics by laser surface treatment. *Surf. Coat. Technol.* 2006, **201**, 3163-3173.

10.- Larrea, A., de la Fuente, G. F., Merino, R. I. and Orera, V. M. ZrO_2-Al_2O_3 eutectic plates produced by laser zone melting*. J. Eur. Ceram. Soc.,* 2002, **22**, 191–198.

11.- Ester, F.J., Merino, R.I., Pastor, J.I., Martin, J., Llorca, J. Surface modification of Al_2O_3-$ZrO_2(Y_2O_3)$ eutectic oxides by laser melting: processing and wear resistance. *Journal of the American Ceramic Society*, 2008, **91**, 3552-3559.

12.- Merino, R. I., Peña, J. I., Laguna-Bercero, M. A., Larrea, A. And Orera, V. M. Directionally solidified calcia stabilised zirconia–nickel oxide plates in anode supported SOFC's. *J. Eur. Ceram. Soc.*, 2004, **24**, 1349–1353.

13.- De Francisco, I. Thesis, University of Zaragoza (2005).

14.- Campana, R., Larrea, A., Peña, J.I. and Orera V.M. Ni–YSZ cermet micro-tubes with textured surface *J. Europ. Ceram. ,* 2009, **29**, 85-90.

15.- Merino, R.I. Cerámicas eutécticas solidificadas direccionalmente para fotónica y electrocerámica, *Rev. Real Academia de Ciencias. Zaragoza*, 2006, **61**, 47-86.

16.- Yoshikawa A, Epelbaum BM, Hasegawa K, Durbin SD, Fukuda T. Microstructures in oxide eutectic fibers grown by a modified micro-pulling-down method. *J Cryst Growth* 1999, **205**, 305-316.

17.- Pei, Y.T. and de Hosson, J. Th.M. Functionally graded materials produced by laser cladding. *Acta Mater,* 2000, **48**, 2617-2624.

18.- Carvalho, P.A. and Vilar, R. Laser alloying of zinc with aluminium: solidification structures. *Surface and Coatings Technology*, 1997, **91**, 158-156.

19.- Laguna-Bercero M.A., PhD Thesis, University of Zaragoza, 2005.

20.- Merino, R.I., de Francisco, I., Peña, J.I. Ionic conductivity in directionally solidified Al_2O_3-ZrO_2(3%mol Y_2O_3) near eutectic composites. *Solid State Ionics* 2007, **178**, 239-247.

21.- Llorca, J. and. Orera, V.M., Directionally solidified eutectic ceramic oxides. *Prog. Mater. Sci*., 2006, **51,** 711.

22.- Kou, S. *Transport Phenomena and Materials Processing*. John Wiley and Sons Inc. New York, 1996.

23.- Mazumder, J. Overview of melt dynamics in laser processing. *Optical Engineering*, 1991, **30**, 1208- 1219.

24.- Page 8.5-13 in reference 22.

25.- Fratello, V.J. and Brandle, C.D. Physical properties of a $Y_3Al_5O_{12}$ melt. *Journal of Crystal Growth*, 1993, **128**, 1006-1010.

26.- Bhat B.N., Effect of thermotransport on directionally solidified aluminium-copper eutectic. *Journal of Crystal Growth*, 1975, **28**, 68-76.

27.- Flemings, M.C. Principles of Control of Soundess and Homogeneity of Large Ingots. *Scandinavian J. Metal.* 1976, **5**, 1-15.

Published in: Journal of the European Ceramic Society 30 (2010) 147–152
doi:10.1016/j.jeurceramsoc.2009.04.031

Table 1. Sizes of the different layers observed on the samples. δ_t =total thickness of the solidified layer, δ_n = thickness of the NiO upper layer, δ_z = thickness of the YSZ layer formed on top of the ceramic substrate.

Traverse speed (mm/h)	δ_t (μm)	δ_n (μm)	δ_z (μm)
20	412	62	19.4
40	364	41	12.8
60	414	27	6.8
100	420	7.2	9
500	495	0	0

Published in: Journal of the European Ceramic Society 30 (2010) 147–152
doi:10.1016/j.jeurceramsoc.2009.04.031

Figures.

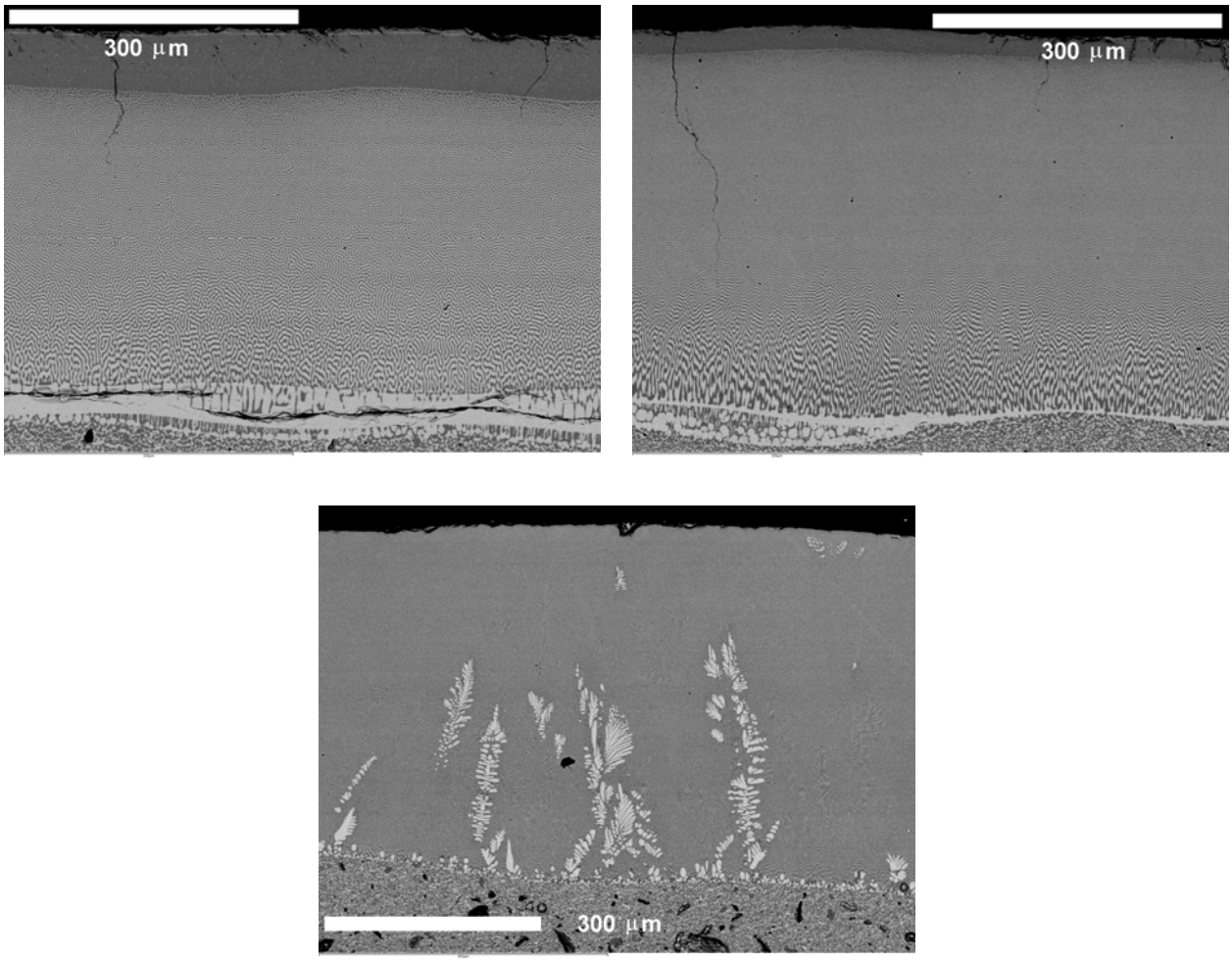

Figure 1. SEM micrographs of polished transverse cross-sections of laser melt samples processed at increasing traverse speeds: a) 20 mm/h; b) 60 mm/h, and c) 500 mm/h. Bright phase: YSZ; dark: NiO.

Published in: Journal of the European Ceramic Society 30 (2010) 147–152
doi:10.1016/j.jeurceramsoc.2009.04.031

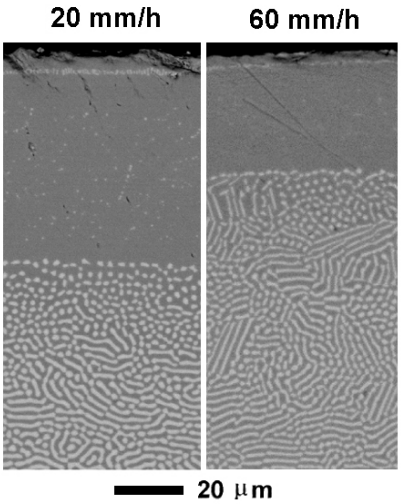

Figure 2. SEM micrographs of polished transverse cross-sections of laser melt samples processed at 20 mm/h (left) and 60 mm/h (right) traverse speeds. Detail near to the surface. Bright phase: YSZ; dark: NiO.

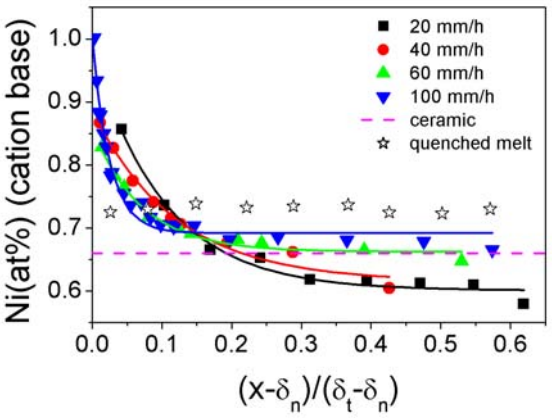

Figure 3. Ni content (Ni atoms over the total cation content) as a function of depth in the solidified layer. The quantification has been made bye EDS using calibration patterns measured ad-hoc. The dotted line indicates the ceramic composition. The stars (☆) the composition of the quenched melt in front of the solid-liquid interface of the layer (crosses in figure 5).

Published in: Journal of the European Ceramic Society 30 (2010) 147–152
doi:10.1016/j.jeurceramsoc.2009.04.031

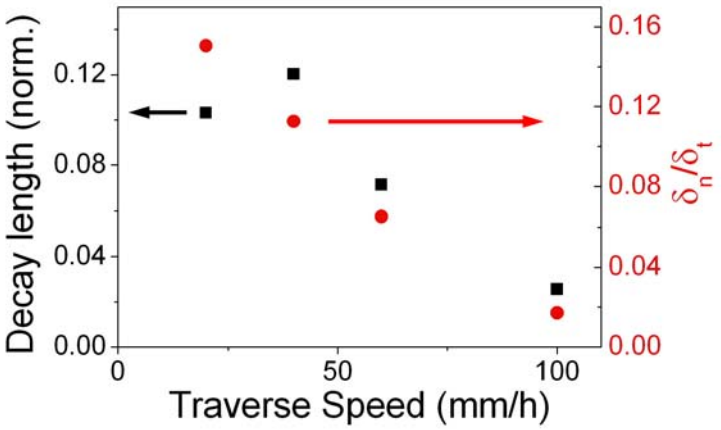

Figure 4. Dependence of normalized decay length (left axis) and of normalized NiO layer thickness (right axis) with laser traverse speed.

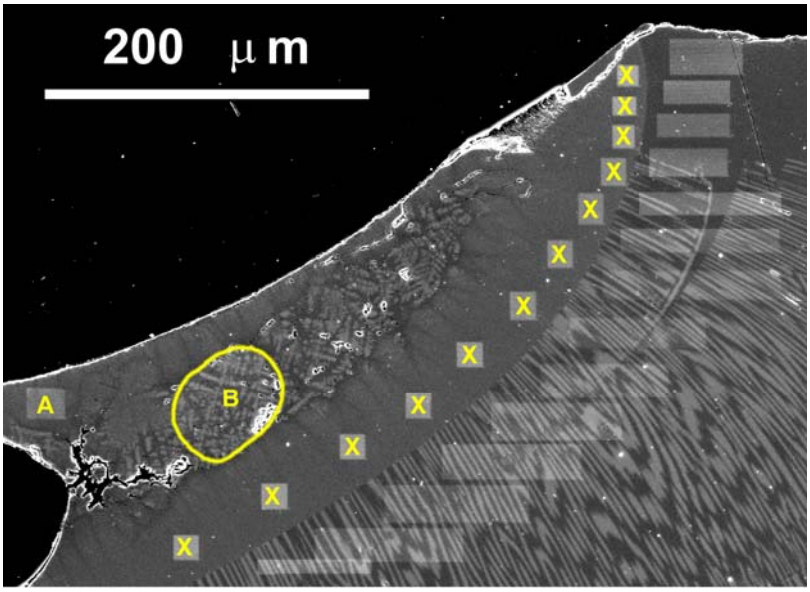

Figure 5. SEM micrograph of a longitudinal cross-section of the quenched melt. The whitened areas marked with an **X** indicates where the EDS cation analyses plotted in figure 3 were made. At **A** the Ni content is 72.6 % cat, at B: 70.3 %.